Colloid Polym Sci (2012) 290:1033–1040
DOI 10.1007/s00396-012-2611-4

ORIGINAL CONTRIBUTION

Monitoring coalescence behavior of soft colloidal particles in water by small-angle light scattering

Dan Wei · Hua Wu · Zhengbin Xia · Delong Xie · Li Zhong · Massimo Morbidelli

Received: 16 December 2011 / Revised: 10 February 2012 / Accepted: 14 February 2012 / Published online: 9 March 2012

Abstract The fractal dimension (D_f) of the clusters formed during the aggregation of colloidal systems reflects correctly the coalescence extent among the particles (Gauer et al., Macromolecules 42:9103, 2009). In this work, we propose to use the fast small-angle light scattering (SALS) technique to determine the D_f value during the aggregation. It is found that in the diffusion-limited aggregation regime, the D_f value can be correctly determined from both the power law regime of the average structure factor of the clusters and the scaling of the zero angle intensity versus the average radius of gyration. The obtained D_f value is equal to that estimated from the technique proposed in the above work, based on dynamic light scattering (DLS). In the reaction-limited aggregation (RLCA) regime, due to contamination of small clusters and primary particles, the power law regime of the average structure factor cannot be properly defined for the D_f estimation. However, the scaling of the zero angle intensity versus the average radius of gyration is still well defined, thus allowing one to estimate the D_f value, i.e., the coalescence extent. Therefore, when the DLS-based technique cannot be applied in the RLCA regime, one can apply the SALS technique to monitor the coalescence extent. Applicability and reliability of the technique have been assessed by applying it to an acrylate copolymer colloid.

D. Wei · H. Wu · Z. Xia · D. Xie · L. Zhong
School of Chemistry and Chemical Engineering,
South China University of Technology,
510640 Guangzhou, Guangdong, China

H. Wu (✉) · M. Morbidelli
Institute for Chemical and Bioengineering, Department of Chemistry and Applied Biosciences, ETH Zurich,
8093 Zurich, Switzerland
e-mail: hua.wu@chem.ethz.ch

Keywords Coalescence · Fractal dimension · Small-angle light scattering · Reaction limited · Diffusion limited · Colloidal aggregation

Introduction

Manufacturing of non-porous polymeric films starts typically from aqueous dispersions of elastomer (soft) colloidal particles, where during the evaporation, upon physical contact, the particles undergo coalescence (complete fusion) as a result of polymer chain interdiffusion or viscous flow [1–4]. Many factors affect the coalescence rate and extent, thus the production process and final properties of the films. Various experimental and theoretical studies have been carried out to understand the effects of surface properties (fixed charges, presence of surfactant, interfacial-tension, etc.), presence of rigid nanodomains, temperature, etc., on the particle coalescence behavior [5–12].

For such colloidal system, due to nano and submicron scales of the primary particles, it is often difficult to observe directly the coalescence process using microscopic tools. An effective technique for monitoring the coalescence should respond in situ and fast to the structure evolution of the clusters, and it should have at least one concrete output indicator (parameter) that clearly reflects the coalescence extent. To this aim, recently, Gauer et al. [5,8] have proposed a technique that combines:

1. Dynamic light scattering (DLS) experiments to monitor diffusion-limited cluster aggregation (DLCA) kinetics of the coalescence system;
2. Simulating the obtained kinetics using the Smoluchowski kinetic approach, based on the population balance equations (PBE), to obtain the fractal dimension of the clusters.

For this technique, it is the fractal dimension that reflects the coalescence extent. In particular, the DLCA process is a rather simple, well-studied physical process, realizable by completely destabilizing the colloidal system using a salt. Since the only transport mechanism for particle collision is diffusion in this case, the sticking probability is close to unity. It is well known that the following PBE can be well applied to the DLCA process [6,13–15]:

$$\frac{dN_i(t)}{dt} = -\sum_{j=1}^{\infty} K_{i,j} N_i N_j + \frac{1}{2}\sum_{j=1}^{i-1} K_{i-j,j} N_{i-j} N_j \quad (1)$$

where $N_i(t)$ is the number concentration of cluster with mass i at time t, $K_{i,j}$ is aggregation rate constant (or kernel) between two clusters with mass i and j, which in the case of DLCA defined as [6,15–17]:

$$K_{i,j} = \frac{K_B}{W}\frac{\left(i^{1/D_f} + j^{1/D_f}\right)\left(i^{-1/D_f} + j^{-1/D_f}\right)}{4} \quad (2)$$

where $K_B = 8kT/3\mu$ is Smoluchowski rate constant (k is Boltzmann constant, T and μ are dispersant temperature and dynamic viscosity, respectively), W is the Fuchs stability ratio with a typical value around 2 under DLCA [5], and D_f is the fractal dimension of the formed clusters. The most important fact is that under DLCA, the D_f value is around 1.8 for rigid non-coalescence particles and equals 3.0 for soft complete coalescence systems [6,7,18]. Thus, if we perform the aggregation under DLCA conditions, each D_f value between the two extremes, 1.8 and 3.0, represents different extent of the coalescence. The key point is that in the above Eqs. 1 and 2, D_f is the only unknown parameter. Therefore, by simulating the measured DLCA kinetics using the above PBE, with D_f as the only fitting parameter, one can understand the coalescence extent among the particles from the obtained D_f value. The validation of this technique has been well done by image analysis of electron micrographs prepared in cryogenic conditions [5].

On the other hand, since the DLCA process requires introducing large amount of salts (sometimes even beyond their solubility in water), the counterion association with the surface charge groups becomes significant, which would change the properties of the particle surface. Then, the observed coalescence behavior unnecessarily represents that of the original system. Thus, it is desirable to monitor the coalescence behavior using small amount of salts, i.e., under the reaction-limited cluster aggregation (RLCA) conditions. However, under RLCA, the aggregation kinetics measured by DLS depends not only on D_f but also on W and λ. The latter is the exponent of a multiplier term, $(ij)^{\lambda}$ for RLCA on the right hand side of Eq. 2, which accounts empirically for the increase of cluster reactivity with size. Although λ should take theoretically a value of about 0.5 [19,20], in reality its value varies between 0 and 0.5, depending on the specific colloidal system, thus often a fitting parameter. Thus, by simulating the RLCA kinetics measured by DLS, one cannot define uniquely the D_f value—the coalescence extent.

To solve the above difficulty, in this work we propose to use the small-angle light scattering (SALS) technique to monitor the kinetics and structure evolution of the clusters under RLCA so as to understand the coalescence extent. The advantages of the SALS technique are (1) extremely fast and (2) applicable to large (several tens or hundreds of microns) clusters. To demonstrate its applicability, here we have applied it to monitor the coalescence behavior of an acrylate copolymer colloid. In addition, as a validation step, we have first investigated its coalescence under DLCA and compared the result with that from the previous technique based on DLS.

Experiments

The colloid system

The investigated colloid system is an acrylate copolymer latex supplied by BASF SE (Ludwigshafen, Germany). It is rather monodisperse, and the radius of primary particles determined by static light scattering (SLS) is R_p=90.0 nm, which is equal to the hydrodynamic radius from DLS. The glass transition temperature of the polymer is ~6 °C. Thus, coalescence may occur at room temperature. The particles are stabilized by surface fixed charges ($-COO^-$ and $-SO_4^-$) and amide groups ($-NH_2$), without using surfactant.

The SALS instrument

The SALS instrument used in this work is Mastersizer 2000 (Malvern, UK). It works in the angle range, θ=0.02–40°, with the wavelength of the incident light, λ_0=633 nm. It has an intensity acquisition frequency of 1,000 s^{-1}, and since it measures the intensity values at all the detecting angles at the same time, for the colloidal systems considered in this work, to obtain the entire intensity curve in the given range of scattering angle, it was found that a duration of only 10 s was needed in each measurement.

For a given particulate system, the measured angle-dependent intensity curves, $I(q)$, when divided by the measured form factor, $P(q)$ of the primary particles, defines the normalized structure factor of the clusters in the system, $\langle S(q)\rangle$, as follows [15,21–23]:

$$\langle S(q)\rangle = \frac{I(q)}{I(0)P(q)} \quad (3)$$

where q is the wave vector [$q = (4\pi n/\lambda_0)\sin(\theta/2)$, with n the refractive index of water], and $I(0)$ is the scattered

intensity at $q=0$. With $\langle S(q)\rangle$, the average radius of gyration of the clusters, $\langle R_g\rangle$, can be determined using the Zimm plot [21,24]:

$$\frac{1}{P(q)\langle S(q)\rangle} = 1 + \frac{1}{3}q^2\langle R_g\rangle^2 \quad \text{, for} \quad q\langle R_g\rangle < 1 \tag{4}$$

Another application of $\langle S(q)\rangle$ is that for sufficiently large clusters, $\langle S(q)\rangle$ scales with q as follows [25]:

$$\langle S(q)\rangle \propto q^{-D_f} \quad \text{for} \quad 1/\langle R_g\rangle << q << 1/R_p \tag{5}$$

Thus, the log–log plot of $\langle S(q)\rangle$ vs. q in the given q range should be a straight line and its slope gives the estimate of the fractal dimension, D_f.

Moreover, it is well known [26] that the scattered intensity at $q=0$, $I(0)$, scales as follows:

$$I(0) \propto \langle i\rangle \propto \left(\frac{\langle R_g\rangle}{R_p}\right)^{D_f} \tag{6}$$

where $\langle i\rangle$ is average number of primary particles per cluster. Thus, the slop of the log–log plot of $I(0)$ vs. $\langle R_g\rangle/R_p$ also gives the estimation of D_f.

The DLCA and RLCA experiments

Both the DLCA and RLCA experiments were conducted at a particle volume fraction, $\phi=2\times10^{-5}$. Since the carboxylic groups are present on the particle surface, an acid solution (HCl) was used to effectively destabilize the colloid. In all the preparations, deionized water was used, which was further purified through a Millipore Simpark column and filtered through 0.1 μm Acrodisc syringe filters (Pall, UK). The aggregation was started by pouring the HCl solution into the colloid, followed by a quick and gentle hand shaking. Note that both the HCl solution and the colloid should be prediluted substantially in order to avoid the effect of local inhomogeneity on the aggregation [16]. After few seconds equilibrium, the aggregating system was immediately (but gently) injected into the SALS cell using a syringe to start in situ monitoring the time evolution of the kinetics and cluster structure.

Results and discussion

Determination of CCC by DLS

To warrant if the process monitored in the SALS cell is under the RLCA or DLCA conditions, we need first to determine the critical coagulant concentration (CCC) for fast aggregation (DLCA). This can be easily done using the DLS technique. In particular, the aggregation process was started at the same particle volume fraction, $\phi=2\times10^{-5}$, but at different HCl concentrations, C_{HCl}, following the same preparation procedure described above. Then, the prepared aggregating system was placed into the vial of a wide-angle light scattering instrument, BI-200SM goniometer system (Brookhaven, USA) equipped with a solid-state laser, Ventus LP532 (Laser Quantum, UK) of wavelength $\lambda_0=532$ nm and started the in situ DLS measurements at $\theta=90^o$, in order to obtain the aggregation kinetics, i.e., the time evolution of average hydrodynamic radius, $\langle R_h\rangle$.

Note that in the case of low HCl concentrations, the aggregation was very slow and the duration is long. To avoid effect of particle sedimentation, for each aggregating system we prepared two vials. One was used for the DLS measurements and another was stored upside down. After a certain defined period, the two vials were turned and exchanged for the measurements [12].

Figure 1 shows the $\langle R_h\rangle$ values as a function of time t at different C_{HCl} values. As can be seen, the rate of the $\langle R_h\rangle$ evolution with time increases as C_{HCl} increases. However, for $C_{HCl}\geq0.125$ mol/L, the aggregation rate becomes independent of C_{HCl}, indicating that the CCC value for the current colloid system is about 0.125 mol/L for HCl. Therefore, the aggregation at $C_{HCl}\geq0.125$ mol/L is under the DLCA conditions, while it is under RLCA for $C_{HCl}<$ 0.125 mol/L.

Moreover, as mentioned in the "Introduction", for the DLCA kinetic data in Fig. 1 at $C_{HCl}\geq0.125$ mol/L, we can apply the PBE with D_f as the only fitting parameter to understand if coalescence among the particles occurs or not, i.e., the technique proposed by Guaer et al. [5,8]. Thus,

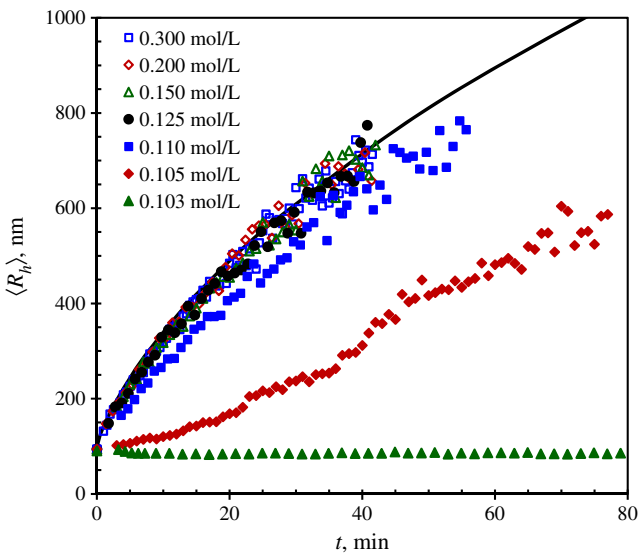

Fig. 1 Time evolution of the average hydrodynamic radius, $\langle R_h\rangle$, determined by in situ DLS, as a function of time, t, at $\phi=2\times10^{-5}$ and different C_{HCl} values, as reported in the legend. The *solid curve* is the PBE simulation of the DLCA kinetics with $D_f=1.75$

we have calculated the time evolution of cluster mass distribution (CMD) (N_i, i=1, 2, …) using Eqs. 1 and 2, with which we have computed the $\langle R_h \rangle$ value, based on [5]:

$$\langle R_h \rangle = \frac{\sum_{i=1}^{\infty} N_i i^2 P_i(q)}{\sum_{i=1}^{\infty} \frac{N_i i^2 P_i(q)}{R_{h,i}}} \quad (7)$$

where $P_i(q)$ and $R_{h,i}$ are the form factor and hydrodynamic radius of individual cluster of mass i. For a spherical cluster, $P_i(q)$ is calculated using the Lorenz–Mie theory and $R_{h,i} = i^{1/3} R_p$ [5]. In the case of a fractal cluster, $P_i(q)=P(q)S_i(q)$, where $P(q)$ is the form factor of the primary particles and $S_i(q)$ the cluster structure factor, whose expression, as well as that for $R_{h,i}$, can be found elsewhere [27]. The simulated time evolution of $\langle R_h \rangle$ is shown in Fig. 1 (solid curve), and the obtained fractal dimension is D_f=1.75. Since the fractal dimension of the DLCA clusters formed by rigid particles are typically around 1.8 [28,29], this result means that under the DLCA conditions, no coalescence occurs during the aggregation for the given colloidal system.

The RLCA kinetic data in Fig. 1 cannot be simulated by the PBE approach to understand the coalescence extent, because, as mentioned in the "Introduction", they involve too many (three) unknown parameters. Thus, under the RLCA conditions, we will apply the proposed SALS technique in the following.

The DLCA process monitored by SALS

Before dealing with the RLCA process, let us first use the SALS technique to monitor the three DLCA processes at C_{HCl}=0.15, 0.20, and 0.30 mol/L in Fig. 1, to see if the SALS technique can give the same conclusion, i.e., no coalescence occurs under DLCA.

Following the procedure for starting the aggregation and SALS measurements described in experimental section, we have obtained the time evolution of the original average structure factor, $I(q)/P(q)$, which in the case of C_{HCl}= 0.15 mol/L is shown in Fig. 2a. It is seen that the power law region of the structure factor develops progressively with time. The bending region of the curve moves towards smaller q values, indicating that the average radius of gyration $\langle R_g \rangle$ of the clusters increases with time. When the original average structure factors in Fig. 2a are normalized, i.e., divided by the corresponding $I(0)$, we obtain the normalized average structure factors, $\langle S(q) \rangle$, which now have been plotted in Fig. 2b as a function of the normalized wave factor, $q \times \langle R_g \rangle$. It is seen that all the $\langle S(q) \rangle$ data at different time collapse into a single curve. This clearly shows that the clusters grow following the fractal scaling, and the well-defined power law region in Fig. 2b gives the fractal dimension, D_f=1.75±0.02, which is consistent with the PBE simulation result of the DLS data, i.e., no coalescence occurs under DLCA for the given colloidal system.

Further confirmation of the obtained D_f value can be done by plotting $I(0)$ vs. $\langle R_g \rangle / R_p$ in a log–log plane, following Eq. 6, which is shown in Fig. 2c. The slope of the plot gives the value for D_f, which is again 1.75. To conclude this subsection, let us now use the same CMD computed previously from Eqs. 1 and 2 using D_f=1.75, to predict the time evolution of $\langle R_g \rangle$, based on the following expression:

$$\langle R_g \rangle^2 = \frac{\sum_{i=1}^{\infty} N_i i^2 R_{g,i}^2}{\sum_{i=1}^{\infty} N_i i^2} \quad (8)$$

where $R_{g,i}$ is the radius of gyration of individual cluster with mass i. For a spherical cluster, $R_{g,i} = (3/5)^{1/2} i^{1/3} R_p$ [12], and for a fractal cluster, its expression can be found elsewhere [30]. The predicted time evolution of $\langle R_g \rangle$ is compared to the experimental data in Fig. 2d, where the $\langle R_h \rangle$ data under DLCA in Fig. 1 are also included. It is seen that the predictions are in good agreement with experiments, again confirming the correctness of the D_f value.

The RLCA process monitored by SALS

Now for the given colloidal system, we perform the aggregation under the RLCA conditions and monitor it using SALS. We still use HCl to destabilize the system but at a concentration, C_{HCl}=0.06 mol/L, which is much lower than the CCC (=0.125 mol/L). The time evolution of the normalized average structure factor, $\langle S(q) \rangle$, are shown in Fig. 3a as a function of the normalized wave vector, $q \times \langle R_g \rangle$. Comparing Fig. 3a under RLCA to Fig. 2b under DLCA, we can observe two distinct differences.

First, in Fig. 2b all the $\langle S(q) \rangle$ data at different time collapse in a single curve, while in Fig. 3a only part of the $\langle S(q) \rangle$ data collapse. Particularly at short aggregation time in Fig. 3a, several data points at large q values are basically flat (i.e., independent of $q \times \langle R_g \rangle$). Since $S(q)$=1 for primary particles, this result means that in the aggregating system there are large amount of the primary particles. This occurs typically for a RLCA process [31], where the reactivity of the clusters increases as their size increases, leading to very broad cluster size distribution. With increase in the aggregation time, the cluster size distribution shifts to larger sizes (smaller q values), and it follows that the uncollapsed points in Fig. 3a decrease.

Second, all the points in Fig. 2b after collapsing form a power law regime in the $q \times \langle R_g \rangle$ range of at least one order of magnitude. This regime allows us to estimate correctly the fractal dimension of the DLCA clusters, D_f=1.75.

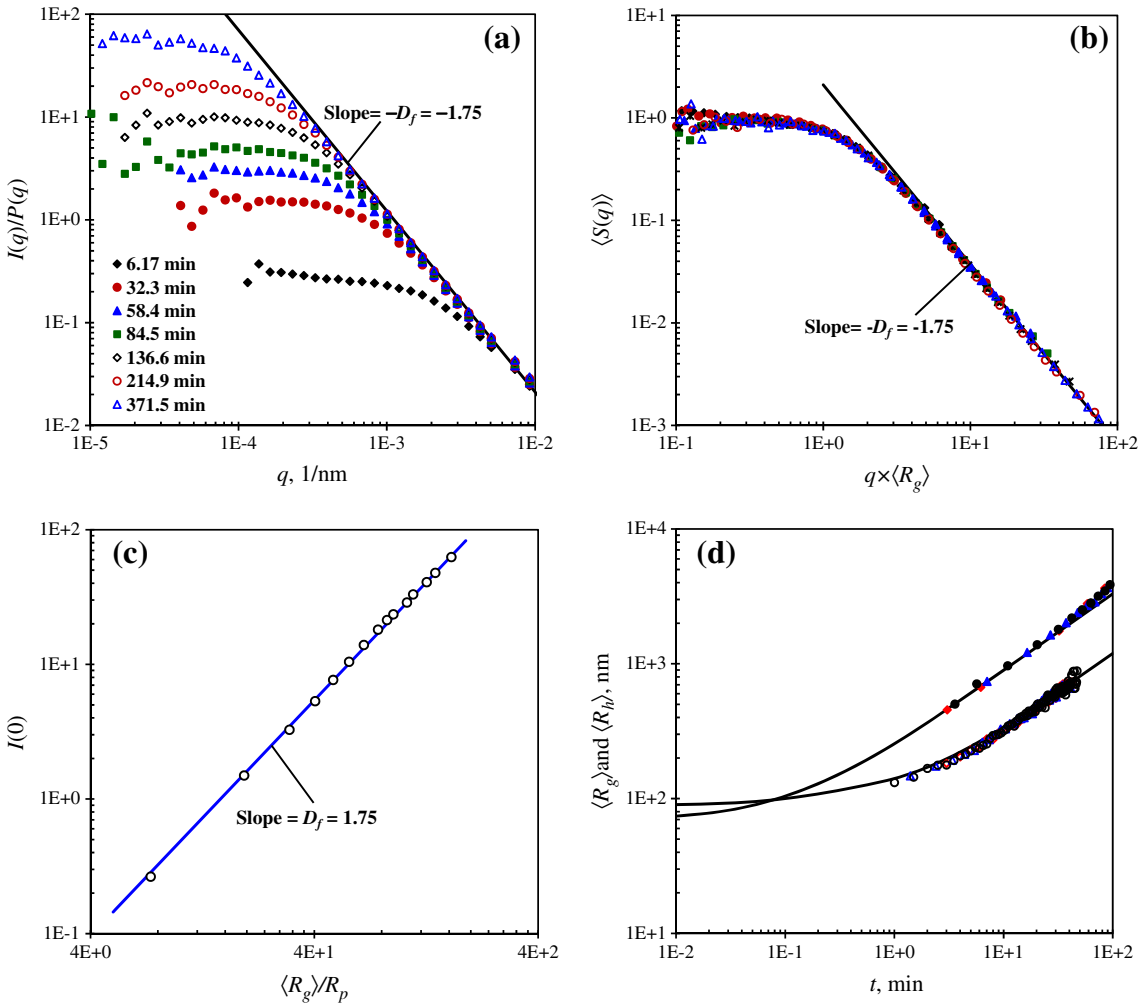

Fig. 2 **a** Time evolution of $I(q)/P(q)$ measured by SALS for the DLCA process at C_{HCl}=0.15 mol/L; **b** normalized average structure factor, $\langle S(q)\rangle$, from the data in **a**, as a function of normalized wave factor, $q\times\langle R_g\rangle$; **c** plot of $I(0)$ vs. $\langle R_g\rangle/R_p$ based on Eq. 6; **d** PBE simulations of the time evolutions of $\langle R_g\rangle$ and $\langle R_h\rangle$ under DLCA with D_f=1.75, compared with experiments. $\phi=2\times10^{-5}$

However, in Fig. 3a, a power law regime cannot be unambiguously defined from the collapsed points. Thus, no D_f value can be determined from Fig. 3a for the RLCA clusters. This arises because of the broad cluster size distribution. Recall that the structure factor of a cluster follow correctly the power law scaling only when the cluster contains more than 50 primary particles or equivalently $R_g/R_p>7$ [30]. Thus, the structure factors of small clusters with $R_g/R_p>7$, together with that of the primary particles, $S(q)=1$, reduce substantially the slope of the power law region of the average structure factor, $\langle S(q)\rangle$. This problem may be solved by performing the aggregation for extremely long time such that $\langle S(q)\rangle$ is dominated substantially by the large, well-developed fractal clusters.

On the other hand, although we cannot estimate the fractal dimension from the $\langle S(q)\rangle$ curves, we may obtain the D_f value from the $I(0)$ vs. $\langle R_g\rangle/R_p$ plot based on Eq. 6 because small clusters with $R_g/R_p>3$ have already followed correctly the $I(0)$ vs. R_g/R_p fractal scaling [30]. Such a plot is shown in Fig. 3b. It can be seen that after the $\langle R_g\rangle/R_p$ value becomes larger than 7, all the data points follow well a straight line in the log–log plane, and the slope leads to the estimate for the fractal dimension of the clusters, D_f=2.66. It is well known [29,32] that the fractal dimension of the clusters formed by rigid particles under the RLCA conditions is around 2.1. Now the obtained D_f value for our clusters is substantially larger than 2.1, which indicates that coalescence occurs for the given colloidal system under the RLCA conditions. Since full coalescence would lead to D_f=3, the D_f value of 2.66 corresponds to a partial coalescence.

It should be mentioned that for single clusters the correct fractal scaling starts at $R_g/R_p>3$ [30], while for the populated system under the DLCA conditions it starts at $\langle R_g\rangle/R_p>4$ in Fig. 3c and under the RLCA conditions it starts at $\langle R_g\rangle/R_p>7$ in Fig. 3b. These results indicate that for a wider cluster mass distribution, the fractal scaling starts at a larger average size of the clusters.

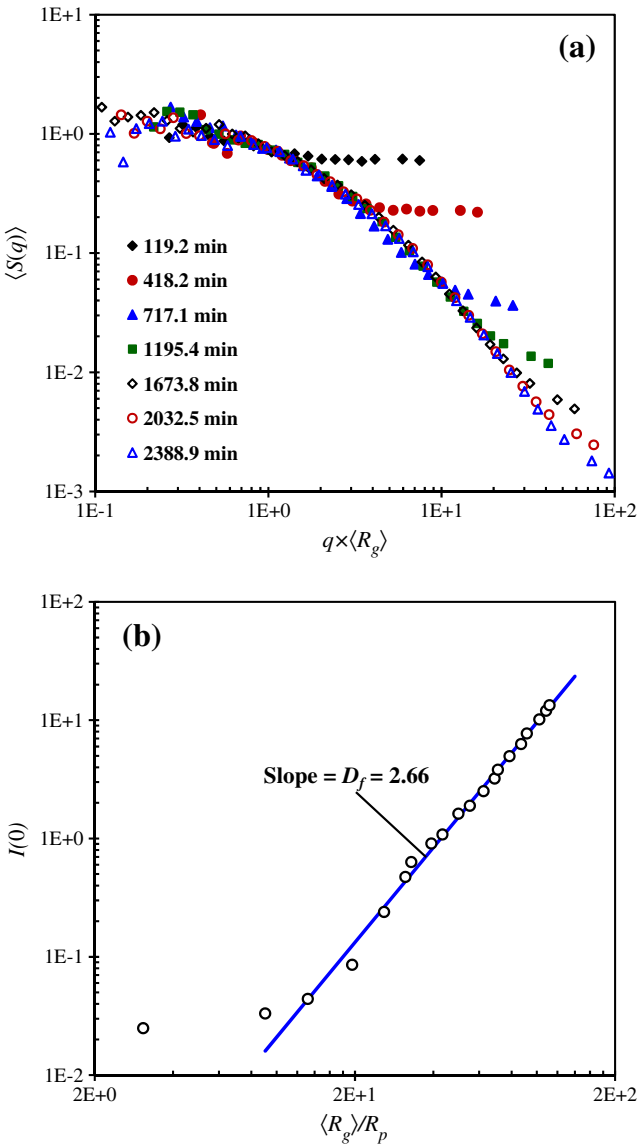

Fig. 3 **a** Normalized average structure factor, $\langle S(q)\rangle$, as a function of normalized wave factor, $q\times\langle R_g\rangle$, obtained at different time for the RLCA process at C_{HCl}=0.06 mol/L; **b** plot of the corresponding $I(0)$ vs. $\langle R_g\rangle/R_p$ based on Eq. 6. $\phi=2\times10^{-5}$

Confirmation of coalescence under RLCA from doublet formation rate

In order to have independent evidence for the occurrence of coalescence under the RLCA conditions for the given colloidal system, we have designed experiments to measure the doublet formation rate, $K_{1,1}$, in the presence of surfactant. The background of such experiments is that one crucial difference between coalescence and non-coalescence systems is that during the aggregation, the total surface area of the particles in the system decreases for the former and remains basically constant for the latter. Then, if an ionic surfactant is adsorbed on the particle surface, when coalescence occurs, the reduction in the total particle surface area changes the surfactant adsorption equilibrium, particularly, more surfactant molecules to be adsorbed on the particles, leading to increase in the colloidal stability. The consequence is that if one measures $K_{1,1}$ at different time, since the total surface area decreases with time, the $K_{1,1}$ value decreases with time as well for a coalescence system, while it remains constant for a non-coalescence one [6,33].

Therefore, to demonstrate the occurrence of coalescence under RLCA, we have added 0.7% (with respect to polymer mass) SDS to the given colloidal system and measured the rate constant for the doublet formation, $K_{1,1}$, at three HCl concentrations, C_{HCl}=0.33, 0.36, and 0.39 mol/L, respectively. Note that after adding the surfactant SDS, the CCC value of the system increases from 0.125 to 0.50 mol/L (data not shown). This is why the three HCl concentrations for RLCA are higher than the CCC before adding SDS.

The technique for determining $K_{1,1}$ is based on measurements of conversion of primary particles to doublets at the very initial stage of the aggregation, using light scattering techniques. Details about the technique require significant space to describe, thus not given here. Interested reader may refer to our previous publications [12,33]. It should be mentioned however that the technique is developed only for two extreme cases, non-coalescence and complete coalescence. For a partial coalescence system, one has to know exactly the coalescence extent, i.e., the exact geometry of the doublet, which is obviously not well defined here. On the other hand, a partial coalescence system should behave between the two extremes. Thus, if we treat the same data by assuming non-coalescence and complete coalescence, respectively, and we obtain the same conclusion, then this conclusion can be applied to the partial coalescence system. Figure 4a, b shows the $K_{1,1}$ values as a function of time at the three HCl concentrations, by assuming non-coalescence and complete coalescence, respectively. As expected, at each given time $K_{1,1}$, i.e., the doublet formation rate, increases as the HCl concentration increases. However, in all the cases, $K_{1,1}$ decreases monotonically with time, no matter if one assumes non-coalescence or coalescence. Then, as discussed above, we can confirm that coalescence does occur for the given colloidal system. Note that we cannot conclude if the coalescence is partial or complete from the $K_{1,1}$ experiments. Thus, the advantage of the SALS experiments proposed above is that it gives the D_f value that indicates coalescence extent.

An additional observation should be mentioned. In the absence of SDS, non-coalescence was observed at C_{HCl}= 0.125 mol/L, while coalescence occurred at C_{HCl}=0.06 mol/L. In the presence of SDS, coalescence occurred even at

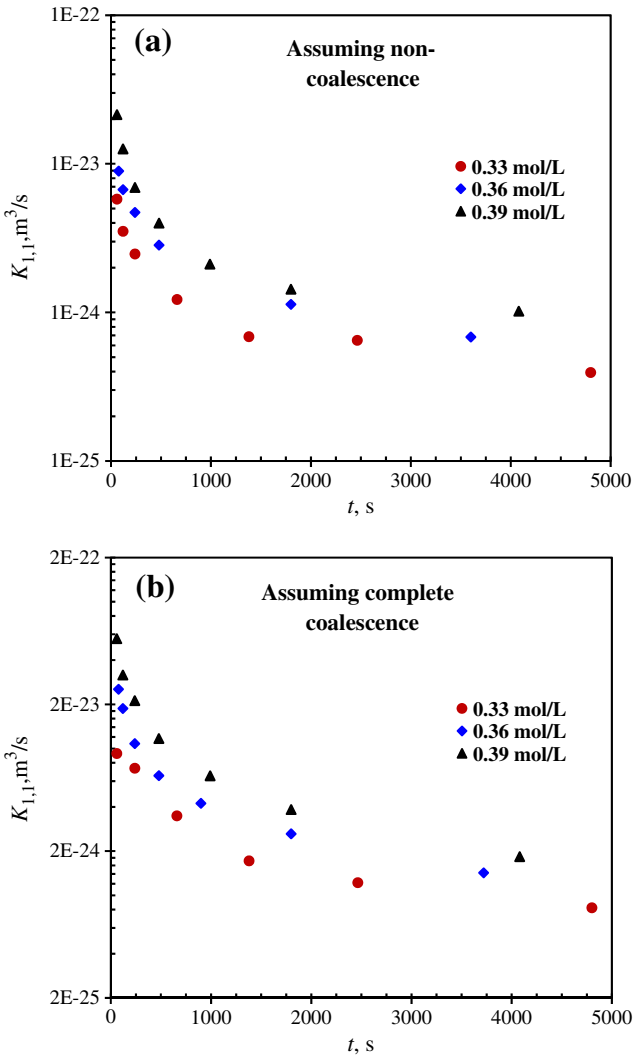

Fig. 4 Doublet formation rate constant, $K_{1,1}$, of the colloid in the presence of 0.7% SDS, evaluated from the initial aggregation kinetics at C_{HCl}=0.33, 0.36, and 0.39 mol/L, respectively, assuming **a** non-coalescence and **b** complete coalescence. $\phi=5\times10^{-2}$

C_{HCl}=0.33 mol/L, which is much larger than 0.125 mol/L. If we exclude any possible effect of SDS on coalescence, these results indicate that whether coalescence occurs or not is independent of the HCl concentration. Instead, it is most likely related to aggregation rate, i.e., at very low aggregation rate (RLCA), coalescence occurs, while at fast aggregation rate (DLCA) non-coalescence occurs. This means that the aggregation and coalescence processes are competing during the aggregation of the given system. Under DLCA, the aggregation process is much faster than the coalescence process, and one cannot observe the occurrence of coalescence. Under RLCA, the coalescence rate becomes comparable or even faster than the aggregation rate, and it follows that significant coalescence has been observed. To verify this point, we have also performed the RLCA experiments at C_{HCl}=0.08 mol/L in the absence of SDS. Since the aggregation rate is increased with respect to that at C_{HCl}= 0.06 mol/L, we should expect less coalescence. In fact, the obtained D_f value is 2.54, smaller than 2.66.

Concluding remarks

We have monitored, using the fast SALS technique, the coalescence behavior of soft acrylate copolymer particles during their aggregation under both reaction-limited and diffusion-limited aggregation (RLCA and DLCA) regimes. Since the fractal dimension, D_f of the clusters formed during the aggregation, reflects correctly the coalescence extent [5], the objective of this work was to assess how one can estimate the D_f value from the SALS experiments.

It is found that under the DLCA conditions the D_f value can be correctly determined from both the power law regime of the average structure factor, $\langle S(q)\rangle$, and the scaling of the zero angle intensity, $I(0)$, vs. the average radius of gyration, $\langle R_g\rangle$. Since $I(0)$ is proportional to the average cluster mass, the latter is the true fractal scaling law. The obtained D_f value is equal to that estimated from the technique based on DLS proposed previously [5].

In the case of RLCA, however, the power law regime of $\langle S(q)\rangle$ cannot be properly defined because of contamination of small clusters and primary particles. Thus, the D_f value cannot be determined from $\langle S(q)\rangle$. On the other hand, the $I(0)$ vs. $\langle R_g\rangle$ plot is still a well-defined straight line in the log–log plane, whose slope gives the estimate of the D_f value, thus the coalescence extent. Therefore, when the DLS-based technique cannot be applied in the RLCA regime, one can apply the SALS technique to monitor the coalescence extent.

For the acrylate copolymer colloid used in this work, it is found that non-coalescence occurs under the DLCA conditions, and partial coalescence takes place under RLCA. In addition, since D_f increases as the coagulant concentration decreases, the coalescence process is competing with the aggregation process. Under DLCA, the aggregation process is much faster than the coalescence process, and one cannot observe the occurrence of coalescence. Under RLCA, the coalescence rate becomes comparable or even faster than the aggregation rate, and it follows that significant coalescence has been observed.

Finally, it should be pointed out that the proposed SALS technique for monitoring the coalescence extent is only applicable to ideal colloidal systems, where rigid bonding occurs during the aggregation. For systems where surface sliding occurs among the particles in the cluster or soft interpenetrating brushes are present on the particle surface, even without coalescence, the fractal dimension can be significantly larger than that of the ideal colloidal systems

under DLCA or RLCA. Thus, for these systems the proposed technique is inapplicable.

Acknowledgments Financial support of BASF SE (Ludwigshafen, Germany), the Swiss National Science Foundation (grant no. 200020-126487/1) and China Scholarship Council are gratefully acknowledged.

References

1. Dobler F, Lambla M, Holl Y (1993) Coalescence mechamisms of polymer colloids. In: Laggner P, Glatter O (eds) Trends in colloid and interface science VII, vol 93. Progress in Colloid and Polymer Science. Springer, New York, pp 51–52
2. Keddie JL (1997) Film formation of latex. Mater Sci Eng R 21 (3):101–170. doi:10.1016/s0927-796x(97)00011-9
3. Steward PA, Hearn J, Wilkinson MC (2000) An overview of polymer latex film formation and properties. Adv Colloid Interf 86(3):195–267. doi:10.1016/s0001-8686(99)00037-8
4. van Tent A, te Nijenhuis K (2000) The film formation of polymer particles in drying thin films of aqueous acrylic latices: II. Coalescence, studied with transmission spectrophotometry. J Colloid Interface Sci 232(2):350–363. doi:10.1006/jcis.2000.7189
5. Gauer C, Wu H, Morbidelli M (2009) Control of coalescence in clusters of elastomer colloids through manipulation of polymer composition. Macromolecules 42(22):9103–9110. doi:10.1021/ma901707s
6. Gauer C, Wu H, Morbidelli M (2009) Effect of surface properties of elastomer colloids on their coalescence and aggregation kinetics. Langmuir 25(20):12073–12083. doi:10.1021/la901702s
7. Gauer C, Wu H, Morbidelli M (2010) Reduction of surface charges during coalescence of elastomer particles. J Phys Chem B 114 (27):8838–8845. doi:10.1021/jp100504k
8. Gauer C, Wu H, Morbidelli M (2010) Coalescence control of elastomer clusters by fixed surface charges. J Phys Chem B 114 (4):1562–1567. doi:10.1021/jp907348e
9. Mazur S, Plazek DJ (2001) Viscoelastic effects in the coalescence of polymer particles. Prog Org Coat 24(1–4):225–236. doi:10.1016/0033-0655(94)85016-x
10. Dobler F, Pith T, Lambla M, Holl Y (1992) Coalescence mechanisms of polymer colloids: I. Coalescence under the influence of particle-water interfacial tension. J Colloid Interface Sci 152(1):1–11. doi:10.1016/0021-9797(92)90002-4
11. Dobler F, Pith T, Lambla M, Holl Y (1992) Coalescence mechanisms of polymer colloids: II. Coalescence with evaporation of water. J Colloid Interface Sci 152(1):12–21. doi:10.1016/0021-9797(92)90003-5
12. Gauer C, Jia ZC, Wu H, Morbidelli M (2009) Aggregation kinetics of coalescing polymer colloids. Langmuir 25(17):9703–9713. doi:10.1021/la900963f
13. Ziff RM, McGrady ED, Meakin P (1985) On the validity of Smoluchowski equation for cluster–cluster aggregation kinetics. J Chem Phys 82(11):5269–5274. doi:10.1063/1.448600
14. HidalgoAlvarez R, Martin A, Fernandez A, Bastos D, Martinez F, delas Nieves FJ (1996) Electrokinetic properties, colloidal stability and aggregation kinetics of polymer colloids. Adv Colloid Interf 67:1–118. doi:10.1016/0001-8686(96)00297-7
15. Wu H, Xie JJ, Morbidelli M (2005) Kinetics of cold-set diffusion-limited aggregations of denatured whey protein isolate colloids. Biomacromolecules 6(6):3189–3197. doi:10.1021/bm050532d
16. Lattuada M, Sandkuhler P, Wu H, Sefcik J, Morbidelli M (2003) Aggregation kinetics of polymer colloids in reaction limited regime: experiments and simulations. Adv Colloid Interf 103(1):33–56. doi:10.1016/s0001-8686(02)00082-9
17. Jia ZC, Wu H, Xie JJ, Morbidelli M (2007) Effect of temperature and surfactant type on the stability and aggregation behavior of styrene-acrylate copolymer colloids. Langmuir 23(20):10323–10332. doi:10.1021/la7013013
18. Prasad SA, Kapoor GP (2011) Fractal dimension of coalescence hidden-variable fractal interpolation surface. Fractals 19(2):195–201. doi:10.1142/s0218348x11005336
19. Axford SDT (1997) Aggregation of colloidal silica: Reaction-limited kernel, stability ratio and distribution moments. J Chem Soc Faraday Trans 93(2):303–311. doi:10.1039/a606195h
20. Lattuada M, Wu H, Sefcik J, Morbidelli M (2006) Detailed model of the aggregation event between two fractal clusters. J Phys Chem B 110(13):6574–6586. doi:10.1021/jp056538e
21. Bohren CF, Huffman DR (1983) Absorption and scattering of light by small particles. Wiley, New York
22. Kerker M (1969) The scattering of light. Academic, New York
23. Brown W (1996) Light scattering—principles and development. Clarendon, Oxford
24. Lindner P, Zemb T (eds) (2002) Neutron, X-rays and light. Scattering methods applied to soft condensed matter. Elsevier, Amsterdam
25. Sorensen CM (2001) Light scattering by fractal aggregates: a review. Aerosol Sci Technol 35(2):648–687. doi:10.1080/02786820117868
26. Wu H, Lattuada M, Sandkuhler P, Sefcik J, Morbidelli M (2003) Role of sedimentation and buoyancy on the kinetics of diffusion limited colloidal aggregation. Langmuir 19(26):10710–10718. doi:10.1021/la034970m
27. Lattuada M, Wu H, Morbidelli M (2003) Hydrodynamic radius of fractal clusters. J Colloid Interface Sci 268(1):96–105. doi:10.1016/j.jcis.2003.07.028
28. Lin MY, Lindsay HM, Weitz DA, Klein R, Ball RC, Meakin P (1990) Universal diffusion-limited colloid aggregation. J Phys Condens Matter 2(13):10.1088/0953-8984/2/13/019
29. Lin MY, Lindsay HM, Weitz DA, Ball RC, Klein R, Meakin P (1989) Universality in colloid aggregation. Nature 339(6223):360–362. doi:10.1038/339360a0
30. Lattuada M, Wu H, Morbidelli M (2003) A simple model for the structure of fractal aggregates. J Colloid Interface Sci 268(1):106–120. doi:10.1016/j.jcis.2003.07.027
31. Sandkühler P, Lattuada M, Wu H, Sefcik J, Morbidelli M (2005) Further insights into the universality of colloidal aggregation. Adv Colloid Interf 113(2–3):65–83. doi:10.1016/j.cis.2004.12.001
32. Lin MY, Lindsay HM, Weitz DA, Ball RC, Klein R, Meakin P (1990) Universal reaction-limited colloid aggregation. Phys Rev A 41(4):2005–2020. doi:10.1103/PhysRevA.41.2005
33. Jia Z, Gauer C, Wu H, Morbidelli M, Chittofrati A, Apostolo M (2006) A generalized model for the stability of polymer colloids. J Colloid Interface Sci 302(1):187–202. doi:10.1016/j.jcis.2006.06.011